

Graph Transformer Networks for Accurate Band Structure Prediction: An End-to-End Approach

Weiye Gong,¹ Tao Sun,² Hexin Bai,³ Jeng-Yuan Tsai,¹ Haibin Ling,^{2,*} and Qimin Yan^{1,†}

¹*Department of Physics, Northeastern University, Boston, MA 02115, USA*

²*Department of Computer Science, Stony Brook University, Stony Brook, NY 11794, USA*

³*Department of Computer and Information Sciences,
Temple University, Philadelphia, PA 19122, USA*

Predicting electronic band structures from crystal structures is crucial for understanding structure-property correlations in materials science. First-principles approaches are accurate but computationally intensive. Recent years, machine learning (ML) has been extensively applied to this field, while existing ML models predominantly focus on band gap predictions or indirect band structure estimation via solving predicted Hamiltonians. An end-to-end model to predict band structure accurately and efficiently is still lacking. Here, we introduce a graph Transformer-based end-to-end approach that directly predicts band structures from crystal structures with high accuracy. Our method leverages the continuity of the k-path and treat continuous bands as a sequence. We demonstrate that our model not only provides accurate band structure predictions but also can derive other properties (such as band gap, band center, and band dispersion) with high accuracy. We verify the model performance on large and diverse datasets.

INTRODUCTION

The electronic structure of solid-state materials is one of the fundamental properties from which multiple physical properties can be derived. Accurate and efficient electronic structure prediction is crucial for understanding complex material functionalities and enabling the data-driven design of functional materials for technological applications. Electronic structures can be characterized in multiple aspects. The first tier includes single-value quantities such as the effective masses, band gaps for nonmetals, and the Fermi energies and work functions for metals. Recent years, the prediction of these single-value properties has been assisted and accelerated by machine learning, more specifically, graph neural networks (GNN) models in crystalline systems to characterize their electronic structures [1–5]. Despite the incorporation of more complex graph structures and extensive physical information, the capability of these models is limited when exploring more intricate applications where predictions beyond single-value targets are needed.

More recently, multiple models have been proposed to predict multi-valued properties of materials, such as the electronic density of states (DOS), to better describe their electronic structures. For instance, the study by Yeo *et al.* [6] treats the DOS as an image-like target that can be learned and subsequently predicted. Mat2Spec [7] employs contrastive learning to encode and align the representations of crystal graph features with the DOS. In a recent work, Xtal2DoS [8] considers DOS as a sequence and employs a graph Transformer to encode the crystal graph, followed by a graph-to-sequence (graph2seq) model serving as a decoder to predict the DOS sequence.

Although DOS can provide simple and explicit information about the electronic structure, the electronic band structure offers a more detailed and explicit representation of crystal properties. Therefore, a machine learning model capable of predicting electronic band structures has become increasingly desirable in recent years.

As an explicit and comprehensive representation of electronic structure, electronic band structures are obtained from first principles calculations which are expensive for complex material systems. For this reason, the prediction of band structures from crystal structures is considered one of the most important tasks in the application of ML to solid-state physics and the data-driven design of functional materials. Recently, an indirect approach has been proposed to train a machine learning model to predict the tight-binding Hamiltonian matrix elements, followed by solving the eigenvalues of the predicted Hamiltonian to obtain the electronic band structure. The approach has been applied to multiple complex material systems, including twisted bilayer graphene and twisted bilayer bismuthene [9] and SiGe alloy systems [10]. In a more recent model, DeepH-E3 [11] integrates GNN with equivariant neural networks (ENN) [12–14], which incorporates specific gauge symmetries in three dimensional space, enabling more data-efficient and accurate model training. However, the investigated material systems are limited to some specific types of material systems. Hence a universal model that can be applied to large scale material datasets is yet to be proposed. Moreover, the need to obtain the eigenvalues of the predicted Hamiltonian with eigenvalue solver limits the scalability and efficiency of these models, thus posing challenges to their practical application in high-throughput material screening.

To address these challenges, we introduce the first end-to-end model *Bandformer* to predict band structures directly from crystal structures. The model is designed based on the architecture of Transformer [15],

* hling@cs.stonybrook.edu

† q.yan@northeastern.edu

Graphormer [16] and Xtal2DoS [8]. We treat the complex relationship between atomic interactions, high symmetry k-paths in reciprocal space, and band energies as a "language translation" task. The crystal structure is encoded into a hidden representation and "translated" into the band structure using a graph2seq module. The model is trained and tested on a large and diverse dataset consisting of 52861 band structures from the Materials Project database [17]. We focus on predicting multiple energy bands around the Fermi level and achieve a mean absolute error (MAE) of 0.14 eV for band energy prediction. We further demonstrate our model's outstanding performance in predicting properties derived from the band structures, achieving a MAE of 72 meV for band center predictions, 84 meV for band dispersion predictions, and 0.164 eV for band gap predictions in non-metals. Our end-to-end model holds great potential in accelerating the data-driven discovery and inverse design of functional materials with specific electronic band structure features.

RESULTS

Theoretical framework of Bandformer

Solving the band structure of crystal systems is a fundamental problem in solid-state physics, essential for understanding material properties. Traditionally, ab initio methods such as density functional theory (DFT) solve the Kohn-Sham eigenvalue equations to obtain these structures. For a typical band structure calculation, crystal structure, atomic potentials and k-point sets are used as input, and band structure is obtained by self-consistent and non-self-consistent calculations are performed to solve eigenvalues at each predefined k-point. Essentially, DFT band structure calculation is a complex mapping between the crystal structure and its band structure, with DFT theory and multiple algorithms applied in the process. According to the universal approximation theorem [18–20], by careful design of model architecture, introducing domain knowledge into the model as a bias and leveraging large datasets, ML models can statistically approximate complex mappings with sufficiently low errors. Hence the central question and core contribution of our work is to investigate whether a machine-learned mapping from crystal structure to band structure can be constructed.

The band structure itself is defined as a piecewise continuous function along high-symmetry paths, represented as a sequence with dimensions $(N_k, 3)$ where N_k denotes the number of k-points sampled. The band structure at these k-points forms a (N_b, N_k) dimensional matrix, where N_b is the number of bands. A critical challenge in developing an ML-based approach for band structure prediction lies in the variability of both N_b and N_k across different materials, as they depend on the crystal's symmetry and electronic configuration. This variability makes the problem unsuitable for direct application of standard

ML models, which typically require fixed input dimensions.

To address the issue of unfixed N_b , we select a fixed number (N) of bands closest to the Fermi level, which are typically the most relevant for determining material properties. For any given crystal, we identify the highest occupied band below the Fermi level and select $N/2$ bands below and $N/2$ bands above this level. To have a consistent and robust definition of band energy, Fermi level is defined as the calculated one for any metal, while shifted to the middle of the band gap for any insulator. This approach ensures that the most critical electronic states are consistently studied across different materials, while maintaining a fixed N_b value.

To address the issue of unfixed N_k , the number of k-points sampled along the high-symmetry path, one may consider padding all to the same length. This is impractical for band structure predictions, where the number of k-points in our dataset can reach up to 1500. Such padding would introduce the computational cost significantly, since the attention mechanism in Transformer-based models scales as $\mathcal{O}(S^2)$ [15]. Hence a smooth resampling of the k-paths is needed. The standard k-path selection in band structure calculation is based on the Setyawan-Curtarolo (SC) scheme [21]. However, this scheme introduce discontinuity in k-paths to avoid repeating, which will make use of discrete continuous data and cause unstable predictions. To generate continuous and moreover, Eulerian k-paths, we use graph theory to add connections between k-points of odd-degree, as is proposed in the Latimer-Munro (LM) scheme [22]. It is necessary for k-paths to be Eulerian to avoid redundant data. Additionally, to handle the imbalanced distribution of sequence lengths across our dataset, we employ a k-point resampling method. This method involves smoothing the band structure using Gaussian interpolation, followed by resampling the k-path to a fixed number of k-points.

While this resampling approach may lead to variations in k-point density along different band structures, it provides a balance between computational efficiency and fidelity. The resampled k-points ensure a consistent input dimension for the ML model, enabling effective learning while minimizing redundant computations. The details of our k-point resampling algorithm and its implications on band structure fidelity are discussed further in Methods section.

The architecture of Bandformer

Fig. 1 shows an overview of Bandformer model workflow and architecture of sub-modules. The essence of our model is treating the band energy prediction task as a language translation task, where the input crystal graph as the input "sentence" is "translated" into the sequence of band energy values as the output "sentence". As shown in Fig. 1 (a), for an input crystal, a typical crystal graph is constructed from local environ-

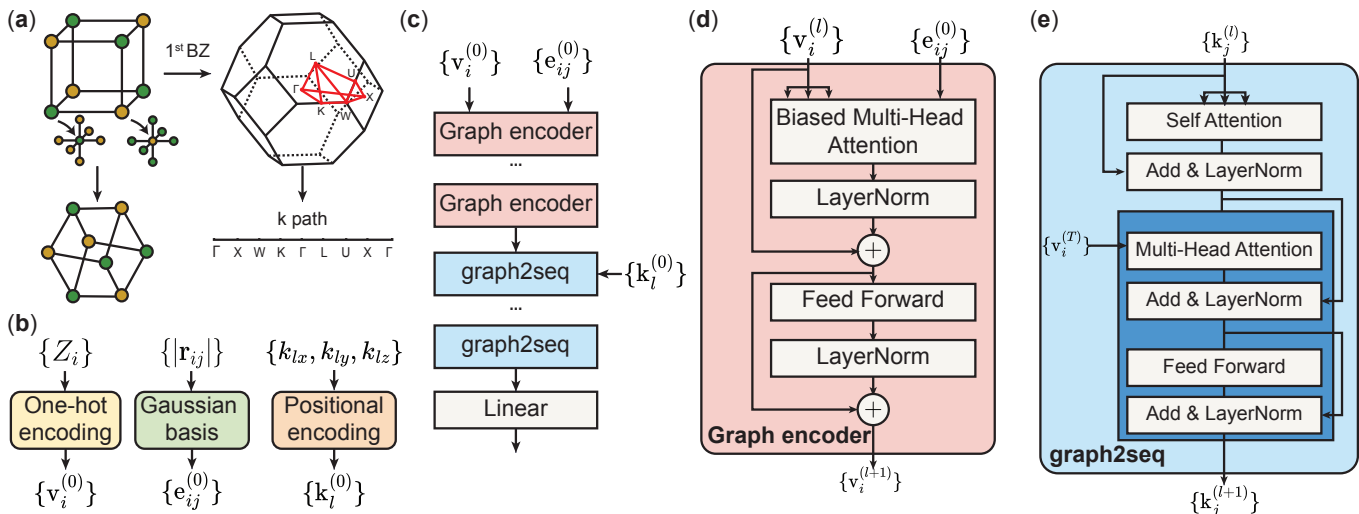


FIG. 1. **The workflow and architecture of Bandformer.** (a) For each input crystal, a crystal graph is constructed from local environment of atoms in the primitive cell, which is used as the input for the encoder. The high symmetry k-path in the first Brillouin zone is extracted and resampled and used as the input for the decoder graph2seq. (b) Atoms are given element features attached to graph nodes, and interatomic distance are given Gaussian expansions of the distance as features. K-points are given spatial positional encoding. (c) The architecture of Bandformer. (d) The architecture of graph encoder. The input atomic features and the edge features are used to generate a bias term when calculating the attention coefficients in the Biased Multi-head Attention module, which is connected to LayerNorm layer in a ResNet structure [23]. (e) For each k-point along high symmetry k-path, positional encoding of k-point coordinates is used as the initial feature, which is passed to a graph2seq decoder. Within the decoder, k-points learn positional information through Self Attention module. The output is passed to the graph2seq attention module, together with the updated graph encoder output.

ment of atoms in primitive cell. Each node represents an atom, and each edge represents the interatomic distance. Each node is then assigned features using one-hot encoding based on its atomic number. Each edge is assigned features defined by Gaussian expansion, which has been commonly used in GNN applied in crystal structures such as CGCNN [1] and SchNet [24]. The continuous k-path following the LM scheme is used as the input for decoder, which will run self attention to learn positional information between k-points and *graph2seq* attention to involve updated crystal graph information. Finally, the predicted band structure is outputted by a output multi-layer perceptron (MLP) layer.

As shown in Fig. 1 (c), the crystal graph is passed to a Graph Transformer encoder to extract hidden representations of nodes by exchanging and updating the graph representations. Edge features are treated as an addition bias term to calculate the attention coefficients, similar to the spatial encoding used in Graphormer [16]. The output of biased multi-head attention module and feed forward module are passed to a skip connection structure known as ResNet [23], which is extensively used in deep neural network models and is one of the most fundamental model architectures. LayerNorm [25] is also used to ensure stable results during the training.

The architecture of decoder is shown in Fig. 1 (e). The real space coordinates combined positional encoding were used for graph transformer for crystals [26], we apply positional encoding of k-points as the initial feature

for the target sequence in the decoder using the same idea. Details can be found in Methods. Next, the data is processed by self-attention module, which helps to identify the relationships among k-points in the sequence. This information is then passed to a *graph2seq* attention module, combined with the graph nodes from the last layer of graph Transformer to calculate *graph2seq* attention coefficients. Finally, the decoder output is passed to a MLP layer to generate the predicted band structure along the specified k-path.

Since the original task of predicting band energies is divided into two sub-tasks, the loss is computed separately for each and combined into a total loss with a weighting factor. Specifically, the total loss is defined as the weighted sum of the MAE loss for the predicted band centers and the MAE loss for the predicted band dispersions, formulated as $\mathcal{L} = \mathcal{L}_1 + \lambda\mathcal{L}_2$, where \mathcal{L}_1 and \mathcal{L}_2 are the MAE loss for predicted band centers and band dispersions correspondingly, and the weighting factor λ is found by hyper-parameter searching algorithm.

A universal model for electronic band structures

We first train and test our model on one of the largest publicly available datasets of band structures, the Materials Project dataset. We select a subset of this dataset which includes band structures for approximately 55,000 unique crystal structures, each calculated using Perdew-

Burke-Ernzerhof (PBE) [27] functionals under line-mode with the VASP code [28–30]. The dataset contains a wide variety of crystal structures, with unit cells varies from 2 to 200 atoms, number of bands varies from 2 to 300, and number of k-points varies from 50 to 2000 points. This diversity provides a robust foundation for model generalizability, enabling the trained model to perform effectively on previously unseen data. Given the variability in number of bands and k-points for structures in the dataset, we standardize them in order to simplify data preprocessing and optimize training efficiency. For a universal k-point selection, two distinct schemes can be used, namely, SC scheme and LM scheme. The schemes defined the k-path by the space group symmetry of the structures to ensure the structures with the same space group symmetry will have the same k-path. As mentioned before, this k-path will have different number of k-points for different structures, which will make data unstructured. To ensure a fixed number of k-points, we first apply a smoothing Gaussian filter function to interpolate the original data points and then resample the band structure using a predetermined number of k-points. The number of resampled k-points is set to 256 for all crystal structures in this work. This process requires a continuous k-path, which is why we use the LM scheme instead of the SC scheme. Although the LM scheme will have redundant k-points, it removes discontinuities in the high-symmetry path, making it suitable for interpolation and resampling. To focus on the bands of greatest interest, we first identify the highest nonempty band and select $N/2$ bands above and $N/2$ bands below it, including itself. N is set to 6 throughout this work and can easily be increased for predicting more bands. The Fermi level remains unchanged for metals, while for non-metals, it is shifted to the middle of the band gap. This ensures more stable training and evaluation of the model. Additional details are provided in the Supplementary Information.

The decoder in our model is based on the Transformer architecture. Since Transformer uses LayerNorm, which applies standard normalization on each band individually, this approach predicts bands with similar value ranges. This makes Transformer more suitable for predicting distribution-like targets, such as phonon DOS and electron DOS. However predicting band structure is more challenging since different bands have different band centers. To address this issue, we decompose the target into two sub-tasks, predicting the band centers and the band dispersions separately. Specifically, the model predicts the mean value (band center) and the deviation from the mean (band dispersion) for each band. The final band structure is then reconstructed by combining these components.

As shown in Fig. 2 (a) and (b), our model achieves a MAE of 72 meV for band center predictions and 84 meV for band dispersion predictions, which are the direct outputs of the model. The MAE metric is employed as it is a standard evaluation criterion in materials science machine learning studies [1, 2, 24]. The predicted

TABLE I. **Model performance on the test set.** Performance is evaluated by MAE loss in electron volts (eV) for band center, band dispersion, band energy, and band gap. Results are provided for the overall test set (Total) as well as separately for non-metal and metal subsets. The band gap is only applicable to non-metals.

Target	Total	Non-metal	Metal
Band center (eV)	0.072	0.071	0.072
Band dispersion (eV)	0.084	0.067	0.103
Band energy (eV)	0.117	0.103	0.133
Band gap (eV)	-	0.164	-

band energy is obtained by summing the predicted band center and band dispersion, enabling direct band structure prediction. In Fig. 3, we visualize the predicted band structures across five quantiles, from Q_1 to Q_5 . The total test set is divided into five groups of equal size, sorted by their MAE loss. Q_1 represents the group with the lowest error, while Q_5 corresponds to the group with the highest error. One representative example from each group is displayed in the figure to illustrate the model’s performance across different error ranges. The results demonstrate that our model can predict electronic band structures with high accuracy using an end-to-end approach, without relying on intermediate quantities. The band structure is generated directly from the model outputs, a task that, to the best of our knowledge, has not been previously achieved.

An additional outcome of our model’s predictions is the determination of the band gap, enabling metal versus non-metal classification. From the predicted band structure, we can directly identify whether a material is metallic or non-metallic and compute the band gap as the difference between the conduction band minimum and the valence band maximum. As shown in Fig. 2 (c), for non-metals, we achieve an MAE of 0.164 eV for band gap predictions, highlighting the model’s capability in this critical application. The results are summarized in Tab I.

DISCUSSION

In this discussion section, we will explore additional results, limitations of our model, and potential future directions for its development. Firstly, it is important to note that our model has limitations, including its inability to predict an unfixed and larger number of bands without prior user selection. To predict a variable number of bands, one approach could be to not fix N_b and identify the maximum N_b value, supplementing with empty virtual bands for materials with fewer actual bands. A similar method could be applied to the number of k-points. For the Materials Project dataset we used, the maximum values for N_b and N_k could be as high as 200 and 1500, respectively. Predicting a 200 by 1500 matrix would require

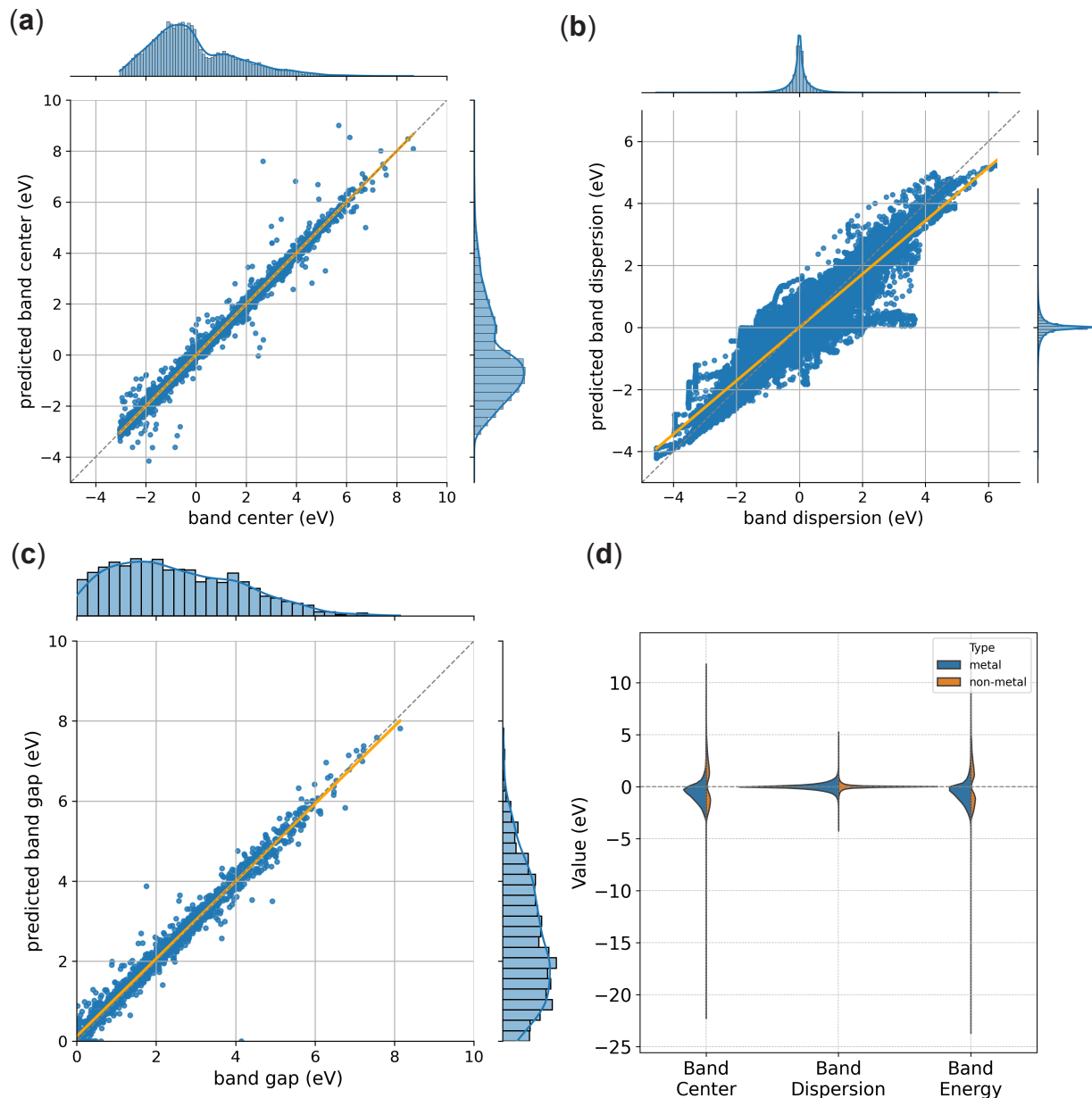


FIG. 2. **Performance of Bandformer on Materials Project band structure dataset.** The scatter plot of predicted vs true (a) band centers, (b) band dispersions (c) band gaps for non-metals. (d) The violin plot of band center, band dispersion and band energy predictions.

substantial computational resources that exceed our current capabilities, but it is not unfeasible. Looking ahead, developing a large-scale model based on Transformer architecture to handle extensive band structure datasets is a promising research direction. Once such a model is trained, it could significantly reduce the computational resources needed for DFT calculations or Hamiltonian solving for a large datasets.

In this work, we limit training to six bands; however, this number can be easily increased by adjusting the model’s hyperparameters and retraining. The current framework allows for straightforward extension to predict

more bands without significant architectural changes. The training cost scales linearly with the number of bands, as the decoder transformer maintains the same output shape, with only the number of neurons in the output MLP layer adjusted to match the required band count. This approach ensures linear time complexity with respect to the number of bands, under the assumption that the distributions of different bands are similar or can be learned from the same underlying data distribution. For a more precise modeling of individual band distributions, a potential improvement would involve using N_b separate graph2seq decoders, each dedicated to learn-

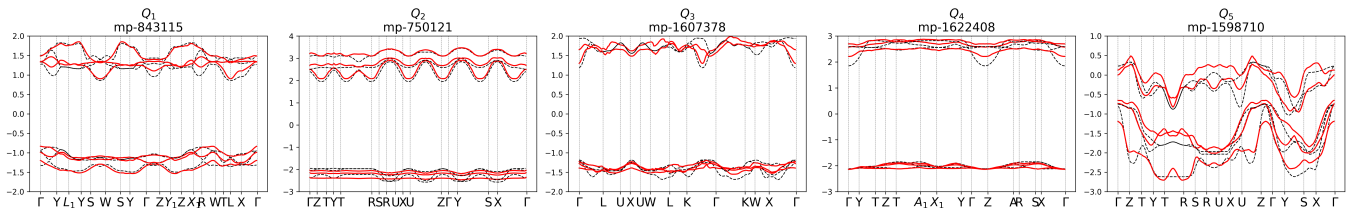


FIG. 3. **Predicted bands (red) vs real bands (black) on Materials Project band structure dataset.** The dataset is divided into five equal sized subsets, with band energy prediction error low (Q_1) to high (Q_5).

ing the unique distribution of a specific band. However, this approach would scale with a complexity of $\mathcal{O}(N_b^2)$, significantly increasing computational costs. Given the strong performance of our current model, we opt to retain the existing architecture, which balances accuracy and efficiency.

Another promising direction for future research involves the extraction of descriptors or targets for band structure-related properties that have more physical meaning, which could enable faster training and enhance model accuracy. In our current work, we applied FFT to convert raw band structure data from reciprocal space to an auxiliary "frequency" space, treating the reciprocal space as "time" space. This transformation produces targets with much smaller dimensions, which helps to reduce oscillations and overfitting in our model predictions. However, the exact physical meaning of this auxiliary space remains unknown, though it may be related to the localization of wave function in real space. Developing a low-dimensional descriptor for crystal band structures that can both decode from and encode into the band structure with minimal information loss would be extremely beneficial. Such a descriptor would simplify the representation of complex band structures, making it easier for models to learn and predict these structures accurately. This approach could significantly improve the performance of models designed for predicting band structures.

METHODS

Graph transformer encoder

For a given input crystal structure, we construct a crystal graph from the atoms in the primitive cell and their neighboring environment, selecting atoms within a predetermined searching radius. We consider 12 nearest neighbors within 8 Å searching radius of each atom to create the crystal graph for each input crystal structure. In the encoding phase, the crystal structure is initially represented as a graph G , where nodes represent atoms, and edges represents interatomic distances. Each vertex i is characterized by a feature vector \mathbf{x}_i^0 based on properties of the atom such as group number, period number and atomic radius. The performance of model using this type

of features is tested and compared to that using just one-hot encoding of atomic number as input features. Each edge ij is represented by a feature vector \mathbf{e}_{ij} , which is a Gaussian function expansion of interatomic distances, which has been used frequently in previous works. We use a graph Transformer architecture within MPNN framework [31]. At each updating step l , edge feature \mathbf{e}_{ij} and atom feature \mathbf{x}_i^l are passed to linear layers without bias to generate edge embedding, query, key and value vectors: $\mathbf{m}_{ij}^l = W_e^l \mathbf{e}_{ij}$, $\mathbf{q}_i^l = W_q^l \mathbf{x}_i^l$, $\mathbf{k}_i^l = W_k^l \mathbf{x}_i^l$, $\mathbf{v}_i^l = W_v^l \mathbf{x}_i^l$, where $\mathbf{e}_{ij}, \mathbf{x}_i \in \mathbb{R}^d$ are d dimensional feature vectors and $W \in \mathbb{R}^{d \times d}$ are $d \times d$ dimensional projection matrices.

Neighboring atoms $\mathcal{N}_r(i)$ within a certain radius r of the center atom i are gathered to calculate the attention coefficients by using *softmax* function defined as

$$\alpha_{ij}^l = \frac{\exp(\langle \mathbf{q}_i^l, \mathbf{k}_j^l; \mathbf{m}_{ij}^l \rangle)}{\sum_{p \in \mathcal{N}_r(i)} \exp(\langle \mathbf{q}_i^l, \mathbf{k}_p^l; \mathbf{m}_{ip}^l \rangle)}, \quad (1)$$

where $\langle \mathbf{q}, \mathbf{k}; \mathbf{m} \rangle = \frac{1}{\sqrt{d}} \mathbf{q}^T \mathbf{k} + \mathbf{m}$ is a modified multi-head scaled dot product with edge feature projection \mathbf{m} included. The node features are updated by a skip connection first introduced in ResNet [23]: $\mathbf{x}_i^{l+1} = \mathbf{x}_i^l + \text{LayerNorm}(\sum_{j \in \mathcal{N}_r(i)} \alpha_{ij}^l \mathbf{x}_j^l)$. After L iteration steps, a crystal feature is obtained by the global pooling of graph nodes $\mathbf{x}^L = \sum_{i \in G} \mathbf{x}_i^L$. This feature serves as the input for the graph2seq decoder.

Reciprocal space positional encoding

In decoding phase, we utilize a graph2seq model similar to Xtal2DoS, which has been used to predict electronic DOS. [8] The output from the encoder is utilized to generate key and value vectors. Each k-point along the k-path has coordinates (k_{ix}, k_{iy}, k_{iz}) . We featurize the k-point coordinates by using the positional encoding defined as:

$$f_n(k_i) = \exp j2\pi\omega_n k_i \quad (2)$$

where

$$\omega_n = \frac{1}{10^{n/(\dim-1)}}, \quad \dim = d_{\text{model}}/6 \quad (3)$$

The feature for a k-point is

$$\text{feat} = [\cos(2\pi\omega_0 k_x), \dots, \cos(2\pi\omega_{\text{dim}-1} k_x), \sin(2\pi\omega_0 k_x), \dots, \sin(2\pi\omega_{\text{dim}-1} k_x), \dots, (\text{repeat for } y \text{ and } z \text{ directions})]. \quad (4)$$

The similar form was been applied to real space coordinates in previous work and proven to be helpful in featurizing coordinate like input [26]. This initial feature is used for generating the query vector for each k-point along the k-paths. x_i^L is used for creating key and value vectors. The initial k-point features, alongside the output from the graph Transformer decoder, are iteratively fed into the decoder for multiple time steps. Finally, the final output from the last layer is processed through a multi-layer perceptron (MLP).

DATA AVAILABILITY

The processed band structure data for model training used in this study is available upon request.

CODE AVAILABILITY

The code of the model used in this study is available upon request.

ACKNOWLEDGMENTS

This work is supported by the U.S. Department of Energy, Office of Science, Basic Energy Sciences, under Award No. DE-SC0023664. This research used resources of the National Energy Research Scientific Computing Center (NERSC), a U.S. Department of Energy Office of Science User Facility located at Lawrence Berkeley National Laboratory, operated under Contract No. DE-AC02-05CH11231 using NERSC award BES-ERCAP0029544.

COMPETING INTERESTS

The authors declare no competing interests.

-
- [1] T. Xie and J. C. Grossman, Crystal Graph Convolutional Neural Networks for an Accurate and Interpretable Prediction of Material Properties, *Phys. Rev. Lett.* **120**, 145301 (2018).
 - [2] C. Chen, W. Ye, Y. Zuo, C. Zheng, and S. P. Ong, Graph Networks as a Universal Machine Learning Framework for Molecules and Crystals, *Chem. Mater.* **31**, 3564 (2019).
 - [3] C. W. Park and C. Wolverton, Developing an improved Crystal Graph Convolutional Neural Network framework for accelerated materials discovery, *Phys. Rev. Materials* **4**, 063801 (2020), arxiv:1906.05267 [cond-mat, physics:physics].
 - [4] K. Choudhary and B. DeCost, Atomistic Line Graph Neural Network for improved materials property predictions, *npj Comput Mater* **7**, 1 (2021).
 - [5] R. Ruff, P. Reiser, J. Stühmer, and P. Friederich, Connectivity Optimized Nested Graph Networks for Crystal Structures (2023), arxiv:2302.14102 [cond-mat, physics:physics].
 - [6] B. C. Yeo, D. Kim, C. Kim, and S. S. Han, Pattern Learning Electronic Density of States, *Sci Rep* **9**, 5879 (2019).
 - [7] S. Kong, F. Ricci, D. Guevarra, J. B. Neaton, C. P. Gomes, and J. M. Gregoire, Density of states prediction for materials discovery via contrastive learning from probabilistic embeddings, *Nat Commun* **13**, 949 (2022).
 - [8] J. Bai, Y. Du, Y. Wang, S. Kong, J. Gregoire, and C. Gomes, Xtal2DoS: Attention-based Crystal to Sequence Learning for Density of States Prediction (2023), arxiv:2302.01486 [cs].
 - [9] H. Li, Z. Wang, N. Zou, M. Ye, R. Xu, X. Gong, W. Duan, and Y. Xu, Deep-learning density functional theory Hamiltonian for efficient ab initio electronic structure calculation, *Nat Comput Sci* **2**, 367 (2022).
 - [10] M. Su, J.-H. Yang, H.-J. Xiang, and X.-G. Gong, Efficient determination of the Hamiltonian and electronic properties using graph neural network with complete local coordinates, *Mach. Learn.: Sci. Technol.* **4**, 035010 (2023).
 - [11] X. Gong, H. Li, N. Zou, R. Xu, W. Duan, and Y. Xu, General framework for E(3)-equivariant neural network representation of density functional theory Hamiltonian, *Nat Commun* **14**, 2848 (2023).
 - [12] T. Cohen and M. Welling, Group Equivariant Convolutional Networks, in *Proceedings of The 33rd International Conference on Machine Learning* (PMLR, 2016) pp. 2990–2999.
 - [13] N. Thomas, T. Smidt, S. Kearnes, L. Yang, L. Li, K. Kohlhoff, and P. Riley, Tensor field networks: Rotation- and translation-equivariant neural networks for 3D point clouds (2018), arxiv:1802.08219 [cs].
 - [14] M. Geiger and T. Smidt, E3nn: Euclidean Neural Networks (2022), arxiv:2207.09453 [cs].

- [15] A. Vaswani, N. Shazeer, N. Parmar, J. Uszkoreit, L. Jones, A. N. Gomez, L. Kaiser, and I. Polosukhin, Attention is All you Need, in *Advances in Neural Information Processing Systems*, Vol. 30 (Curran Associates, Inc., 2017).
- [16] C. Ying, T. Cai, S. Luo, S. Zheng, G. Ke, D. He, Y. Shen, and T.-Y. Liu, Do Transformers Really Perform Bad for Graph Representation? (2021), arxiv:2106.05234 [cs].
- [17] A. Jain, S. P. Ong, G. Hautier, W. Chen, W. D. Richards, S. Dacek, S. Cholia, D. Gunter, D. Skinner, G. Ceder, and K. A. Persson, Commentary: The Materials Project: A materials genome approach to accelerating materials innovation, *APL Materials* **1**, 011002 (2013).
- [18] G. Cybenko, Approximation by superpositions of a sigmoidal function, *Mathematics of control, signals and systems* **2**, 303 (1989).
- [19] K. Hornik, M. Stinchcombe, and H. White, Multilayer feedforward networks are universal approximators, *Neural networks* **2**, 359 (1989).
- [20] T. Chen and H. Chen, Universal approximation to nonlinear operators by neural networks with arbitrary activation functions and its application to dynamical systems, *IEEE transactions on neural networks* **6**, 911 (1995).
- [21] W. Setyawan and S. Curtarolo, High-throughput electronic band structure calculations: Challenges and tools, *Computational Materials Science* **49**, 299 (2010).
- [22] J. M. Munro, K. Latimer, M. K. Horton, S. Dwaraknath, and K. A. Persson, An improved symmetry-based approach to reciprocal space path selection in band structure calculations, *npj Comput Mater* **6**, 1 (2020).
- [23] K. He, X. Zhang, S. Ren, and J. Sun, Deep Residual Learning for Image Recognition, in *2016 IEEE Conference on Computer Vision and Pattern Recognition (CVPR)* (IEEE, Las Vegas, NV, USA, 2016) pp. 770–778.
- [24] K. T. Schütt, H. E. Sauceda, P.-J. Kindermans, A. Tkatchenko, and K.-R. Müller, SchNet – A deep learning architecture for molecules and materials, *The Journal of Chemical Physics* **148**, 241722 (2018).
- [25] J. L. Ba, Layer normalization, arXiv preprint arXiv:1607.06450 (2016).
- [26] Y. Cui, K. Chen, L. Zhang, H. Wang, L. Bai, D. Elliston, and W. Ren, Atomic Positional Embedding-Based Transformer Model for Predicting the Density of States of Crystalline Materials, *J. Phys. Chem. Lett.* , 7924 (2023).
- [27] J. P. Perdew, K. Burke, and M. Ernzerhof, Generalized gradient approximation made simple, *Phys. Rev. Lett.* **77**, 3865 (1996).
- [28] G. Kresse and J. Hafner, Ab initio molecular dynamics for liquid metals, *Phys. Rev. B* **47**, 558 (1993).
- [29] G. Kresse and J. Furthmüller, Efficiency of ab-initio total energy calculations for metals and semiconductors using a plane-wave basis set, *Computational Materials Science* **6**, 15 (1996).
- [30] G. Kresse and J. Furthmüller, Efficient iterative schemes for ab initio total-energy calculations using a plane-wave basis set, *Phys. Rev. B* **54**, 11169 (1996).
- [31] J. Gilmer, S. S. Schoenholz, P. F. Riley, O. Vinyals, and G. E. Dahl, Neural Message Passing for Quantum Chemistry (2017), arxiv:1704.01212 [cs].